JOURNAL OF Applied Polymer SCIENCE

Special Issue: Sustainable Polymers and Polymer Science Dedicated to the Life and Work of Richard P. Wool

Guest Editors: Dr Joseph F. Stanzione III (Rowan University, U.S.A.)
and Dr John J. La Scala (U.S. Army Research Laboratory, U.S.A.)

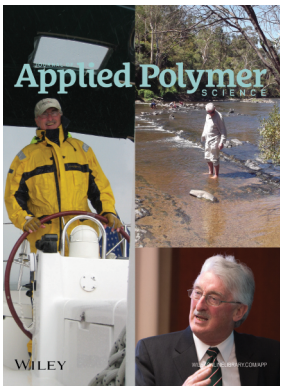

EDITORIAL

REVIEWS

RESEARCH ARTICLES

JOURNAL OF Applied Polymer SCIENCE

Special Issue: Sustainable Polymers and Polymer Science Dedicated to the Life and Work of Richard P. Wool

Guest Editors: Dr Joseph F. Stanzione III (Rowan University, U.S.A.)
and Dr John J. La Scala (U.S. Army Research Laboratory, U.S.A.)

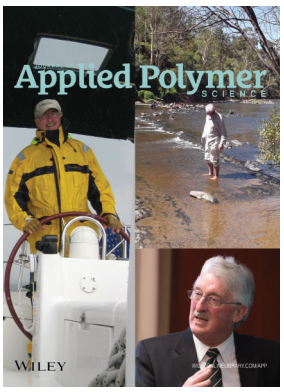

Journal of Applied Polymer Science

Statistical analysis of the effects of carbonization parameters on the structure of carbonized electrospun organosolv lignin fibers

Vida Poursorkhabi,[1,2] Amar K. Mohanty,[1,2] Manjusri Misra[1,2]

[1]School of Engineering, College of Physical & Engineering Science, University of Guelph, Guelph, Ontario, Canada N1G 2W1

[2]Bioproducts Discovery and Development Centre (BDDC), Crop Science Building, Department of Plant Agriculture, University of Guelph, Guelph, Ontario, Canada N1G 2W1

Correspondence to: M. Misra (E-mail: mmisra@uoguelph.ca)

ABSTRACT: Organosolv process is among the top choices for pretreatment of lignocellulosic biomass in cellulosic ethanol production. The lignin obtained as coproduct of this process is a low molecular weight biopolymer. Development of high-value application for this material enhances the economic viability of the bioethanol production process. In this study, aqueous sodium hydroxide solution of organosolv lignin/poly(ethylene oxide) (PEO) blend with 95/5 wt % ratio was electrospun. The fiber morphology and thermal properties were compared with organosolv lignin/PEO fibers electrospun from *N*,*N*-dimethylformamide (DMF) solution. Although organosolv lignin powder and fibers spun from DMF had a low T_g (~100 °C), the fibers from alkaline aqueous solutions did not exhibit a glass transition point and could be carbonized without thermostabilization. The effects of carbonization heating rate, temperature, and time on the average fiber diameter, Raman peaks, and X-ray diffraction results of the carbonized electrospun fibers were statistically analyzed by using a two-level factorial design of experiments. Carbonization temperature, time, and interaction of these two parameters have the most significant effects. Formation of graphitized structures in the carbonized fibers was confirmed by transmission electron microscopy (TEM). The alkaline aqueous electrospinning of organosolv lignin has the advantages of using a green solvent, ability to increase the lignin content of fibers to more than 95 wt %, and removing the time and energy intensive step of thermostabilization before carbonization. © 2016 Wiley Periodicals, Inc. J. Appl. Polym. Sci. **2016**, *133*, 44005.

KEYWORDS: biopolymers & renewable polymers; electrospinning; fibers; glass transition; porous materials

Received 9 January 2016; accepted 31 May 2016

DOI: 10.1002/app.44005

INTRODUCTION

Addition of bioethanol to vehicle fuel has been mandated due to its positive impacts on environment, reduced dependence on fossil fuels, and engine performance.[1] Second-generation bioethanol, also known as cellulosic ethanol, is produced by conversion of polysaccharides from a wide range of lignocellulosic material.[2,3] Cellulose and hemicellulose are covered by lignin which is an irregular aromatic phenolic polymer.[1,4,5] Several physical, chemical, and biological pretreatment processes have been developed to break and separate lignin in order to make cellulose accessible to hydrolyzing enzymes. Among different pretreatments, organosolv process is one of the highly investigated and promising methods.[6,7]

Organosolv process was first developed to avoid air and water pollution in pulp/paper industries in the 1970s. Later, this process was studied for biomass pretreatment in biofuel production.[8] In organosolv process, a mixture of organic solvents is percolated through the biomass. This separates almost all of the extractable material mainly lignin and hemicellulose.[1,6,8] From economic perspective, pretreatment step has the highest contribution (around 18%) to the total production cost of cellulosic ethanol. Organosolv process provides the opportunity for solvent recovery by distillation. The most commonly used solvent is ethanol due to its low toxicity. However, the current technologies for ethanol recovery require a significant amount of energy which increases the process cost. Therefore, economic viability of organosolv process as well as cellulosic ethanol production highly depends on utilizing the coproducts in high-value applications.[6,9–12] Currently, produced lignin during cellulosic ethanol production is burned to produce energy for the process. The excess of lignin (~60 wt %) can be used in higher value applications.[5,13] Research and development has been going on to use lignin for production of carbon fibers as a way to increase the revenue of cellulosic ethanol process, as well as developing a renewable resource-based and low-cost alternative for polyacrylonitrile (PAN)-based carbon fibers in specific applications.[14,15]

© 2016 Wiley Periodicals, Inc.

Organosolv lignins have a structure very similar to native lignins with high purity and homogeneity. They have a high quantity of phenolic and aliphatic hydroxyl groups, low molecular weight, low ash content, and low glass transition point.[1,5]

Lignin fibers have been produced by melt spinning and electrospinning to be used as precursors for carbon fiber production.[14,16] Electrospinning is an electrostatically driven spinning to produce fibers with submicron to nanometer diameters.[17,18] Electrospun lignin-based fibers have been produced as precursors for carbon nanofibers which have been studied for applications in energy storage devices.[19–25]

In the literature, electrospun lignin-based fibers have been produced from blends of kraft lignin/poly(ethylene oxide) (PEO),[26–28] alkali lignin/PAN,[25,29–31] and organosolv lignin in organic solvents. Organosolv lignins have been electrospun by two different approaches. One is electrospinning of solution blends of organosolv lignin and a binder polymer mostly in *N*,*N*-dimethylformamide. Most frequently used binder polymers are PEO[24,26] and PAN.[32,33] The other approach is utilizing co-electrospinning with lignin solution in ethanol as core and ethanol as shell solution.[34] While most of the lignin-based fibers are spun from solutions in DMF, electrospinning of aqueous solutions of lignin has been limited to alkali and kraft lignins. Distilled water and aqueous sodium or potassium hydroxide solutions have been used as a solvent for electrospinning of blends of alkali lignin/PEO,[35] alkali lignin/poly(vinyl alcohol) (PVA),[18,27] kraft lignin/PEO,[36] and alkali lignin/soy protein/PEO.[37] Organosolv lignins are also soluble in aqueous alkali hydroxide solutions and therefore can benefit from an aqueous solution for spinning.

Electrospun lignin-based fibers are often produced as precursors for carbon fiber production. Carbonization of the fibers is usually a two-step thermal process. First step is thermostabilization which is a thermal oxidation of the material by slowly heating the sample in air. The purpose is to increase or remove the glass transition point of the material. This step is crucial to prevent fusion and merging of the fibers at the points they contact each other. Carbonization is the second step in which the sample is heated in an inert atmosphere at a higher heating rate to temperatures more than 800 °C. During this step the carbonized structure is formed.[38,39]

Electrospun organosolv lignin-based fibers require longer thermostabilization times to avoid their fusion compared with kraft and alkali lignins. The successful conditions have been heating rate of 0.05,[40] 0.08,[20] 0.2,[33] 0.25[34] °C/min to 200 °C and holding time at final temperature for 12,[33] 24,[34] and 36 h.[20,40] Organosolv lignin-based fibers thermostabilized at 200 °C with a rate of 1 °C/min and maintained isothermal at maximum temperature for 2 h were fused and interconnected when PEO content increased to 10%.[24] Organosolv lignin/cellulose acetate blend fibers melted when thermostabilized by heating to 300 °C at a rate of 2 °C/min and isothermal time of 2 h. The fiber fusion was controlled and prevented by an iodine treatment.[41] In contrast, alkali lignin-based fibers were thermostabilized at 1 °C/min,[25] modified kraft lignin-based fibers were thermostabilized at 5 °C/min.[27] Therefore, improvement of thermostabilization process of organosolv lignin-based fibers would increase the feasibility of using this lignin for carbon fiber production.

Table I. Two Levels of the Parameters Studied by Design of Experiments

Variable	Symbol	Lower and higher levels
Heating rate (°C/min)	x_1	2–7
Carbonization temperature (°C)	x_2	800–1100
Carbonization time (h)	x_3	3–10

Carbonization of the electrospun lignin-based fibers have been performed at 900, 1000, or 1200 °C with a rate of 10 °C/min and isothermal time at maximum temperature for 0, 1, or 2 h,[20,22,24,25,27,34] or a heating rate of 5 °C/min to 1000 °C and holding for 0.5 h.[33] There are few studies which reported the effects of carbonization temperature for electrospun lignin-based fibers. Ruiz-Rosas *et al.*[40] compared microstructure of the carbonized electrospun Alcell lignin fibers produced at 600, 800, 900, and 1000 °C and a heating rate of 10 °C/min. Schreiber *et al.*[41] compared carbonized organosolv lignin-based fibers produced at 600, 800, 1000, and 1200 °C at a rate of 2 °C/min and held isothermal for 2 h. Another study compared carbonized kraft lignin-based fibers produced at 600, 800, and 1000 °C and holding time of 1 h.[42] These studies compared microstructure of fibers carbonized at multiple temperatures. However, in addition to differences in the type of binder polymer and fiber composition, they used different heating rate and holding times. Therefore, the effects of carbonization temperature observed in one study may not be reproduced in another work.

Organosolv lignin and PEO are soluble in aqueous sodium hydroxide solution and create a highly entangled network which enables reduction of required PEO for spinning.[36] In this study, electrospun organosolv lignin/PEO fibers were produced from an aqueous sodium hydroxide solution. The fibers were thermostabilized at a faster rate than reported rates in the literature for organosolv lignin. Carbonization of both as-spun fibers and thermostabilized fibers was tested. The organosolv lignin/PEO solutions in DMF were also electrospun. For comparison, feasibility of thermostabilization of the latter fibers at the same heating conditions was studied. An in-depth analysis on the effects of carbonization parameters on the microstructure of carbonized electrospun fibers was performed by using a factorial design of experiments. The effects of carbonization temperature, heating rate and holding time on the microstructure of the carbonized O.L./PEO fibers were statistically analyzed. Diameter of carbonized fibers, Raman peak characteristics, XRD data, and TEM images were studied.

DESIGN OF EXPERIMENTS

A two-level factorial design of experiments was used to study the effects of three main carbonization parameters. The parameters were: (a) heating rate, (b) carbonization temperature, (c) carbonization time. The two levels of each parameter and the factorial design of experiments are presented in Tables I and II, respectively.

Table II. Two-level Factorial Design of Experiments for Carbonization of the Electrospun Lignin Fibers (Nonrandomized Order)

	Coded values			Uncoded values		
No.	Heating rate (x_1)	Carbonization temperature (x_2)	Carbonization time (x_3)	Heating rate, x_1 (°C/min)	Carbonization temperature, x_2 (°C)	Carbonization time, x_3 (h)
1	−1	−1	−1	2	800	3
2	1	−1	−1	7	800	3
3	−1	1	−1	2	1100	3
4	1	1	−1	7	1100	3
5	−1	−1	1	2	800	10
6	1	−1	1	7	800	10
7	−1	1	1	2	1100	10
8	1	1	1	7	1100	10
9	0	0	0	4.5	950	6.5

The two levels of heating rate were 2 and 7 °C/min which were lower than the commonly used heating rate of 10 °C/min. Selection of lower heating rates was to study whether slow heating affects the extent of ordered structure. The two levels of temperature were 800 and 1100 °C. The lower limit was selected in agreement with the literature and based on the minimum temperature required to carbonize lignin. The upper temperature was limited by the physical capability of the furnace used in this study as well as temperatures higher than 1100 °C are known for graphitization. Carbonization time which is the residence time of fibers at the carbonization temperature was selected much longer than the literature values which have been selected as 1 or 2 h. In this study, 3 and 10 h were selected. Although 10 h carbonization time increases the energy requirements of the process, it was selected as a high value to exhibit the effects of time.

Design of experiments and statistical analysis of the data were performed by Minitab® 17 software. Confidence level was selected as 95%.

The studied responses were diameter of the carbonized fibers, characteristics of the Raman peaks, and the interlayer spacing of (002) crystallographic planes calculated by XRD. For diameter analysis, 100 measurements were done for each sample. The measurements were divided in five groups of 20 measurements. Average of each group was entered as a replicate. For Raman analysis, three measurements were done for each sample and the data were entered as three replicates. For XRD, one measurement was done for each sample. Significant variables are reported by demonstrating corresponding Pareto charts. For the variables which are close to the significant line of Pareto chart, half normal plots were examined to confirm and the results are reported.

EXPERIMENTAL

Materials

Organosolv hardwood lignin (O.L.) ($M_w = 1551.7$ g/mol, Average moisture content = 3.16 ± 0.36 wt %) was received from Lignol Innovations Ltd. (British Columbia, Canada). Poly(ethylene oxide) (PEO) with $M_v = 2{,}000{,}000$ g/mol was purchased from Sigma-Aldrich Canada Co. Sodium hydroxide (NaOH), *N*,*N*-dimethylformamide (DMF), and ethyl alcohol (EtOH) were purchased from Fisher Scientific Company, Canada. All the materials were used as received. Distilled water was used as the solvent.

Solution Preparation and Electrospinning

Alkaline Aqueous Solution of O.L./PEO. First, separate solutions of lignin and PEO were prepared by dissolving 2.5 g (dry weight) O.L. powder in 15 mL of 0.5 M aqueous sodium hydroxide solution, and 0.13 g PEO in 15 mL distilled water. Both solutions were stirred at 70 to 75 °C and ~600 rpm for 1 h. Then, 8 mL of each solution was transferred to an empty beaker and 4 mL ethanol was added to obtain solutions of 7 wt % (O.L./PEO: 95/5 wt/wt %) in a mixture of alkaline water/ethanol: 80/20 vol/vol %. The NaOH/O.L. weight ratio in the final solution mixtures was about 0.12. The mixed solution was stirred gently for 5 to 7 min before spinning. Prolonged stirring, insufficient heating, or high stirring intensity of the solutions may lead to gelation of the mixture.36 Figure 1 shows the steps for preparing the solutions.

Solution of O.L./PEO in DMF. 0.2 g PEO was dissolved in 20 mL DMF and stirred at 70 °C for 1 h. Then 3.8 g O.L. powder was added and stirred for 1 h. The O.L./PEO ratio in the solution was 95/5 wt/wt %. The total polymer content was

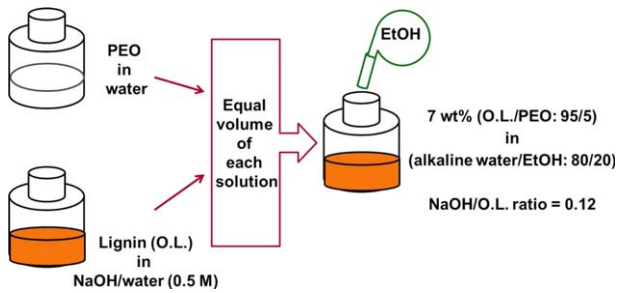

Figure 1. Schematic of steps for preparing the 7 wt % (O.L./PEO: 95/5) solution in a mixture of alkaline water/ethanol:80/20 for electrospinning. [Color figure can be viewed in the online issue, which is available at wileyonlinelibrary.com.]

increased to 20 wt % which was higher than polymer content of alkaline aqueous solutions to achieve a continuous spinning.

A NANON-01A (MECC Co., Japan) electrospinning instrument was used to spin the solutions. The voltage was kept constant at 20 kV. The feed rate was about 0.7 mL/h and was further adjusted to obtain a continuous and steady flow of spinning. The fibers were collected on a stationary flat plate covered with aluminum foil located at a distance of 22 cm from the needle. A 24-gauge needle was used throughout the experiments. The O.L./PEO fibers spun from mixture of aqueous sodium hydroxide and ethanol solution are shortly named as O.L./PEO/aq NaOH and the O.L./PEO fibers spun from DMF solution are named as O.L./PEO/DMF.

Carbonization of the Electrospun Fibers

Collected fibers were cut into pieces and placed in ceramic boats for thermal treatments in furnace. Thermostabilization of the fibers was done in a SentroTech, STT—1200 °C horizontal tube furnace. Two ends of the tube were closed with fittings that had a small opening for air.

Before carbonization experiments for statistical analysis of the parameters, the O.L./PEO/aq NaOH fibers were thermostabilized at 250 °C with a heating rate of 0.5 °C/min and isothermal time for 2 h.[43,44]

Carbonization of the fibers was performed in a Carbolite, GHA—1200 °C horizontal tube furnace. The tube diameter was 7 cm and was continuously purged with nitrogen (~2 L/min). The carbonization conditions are presented in Table II. The yield percentage was calculated by dividing the weight of residual material by the initial weight.

Electrospun fibers were collected with random orientation and during carbonization the fibers were free without external stretching or stress effects. Constraining the sides of the samples could cause different effects in individual fibers based on their alignment with the direction of the restrained sides and it could interfere with the effects of carbonization thermal parameters.

Characterization

Microscopy. A Hitachi S-570 scanning electron microscope (Hitachi High Technologies, Tokyo, Japan) was used at an accelerating voltage of 10 kV. Before imaging, samples were coated with gold/palladium in an Emitech K550 sputtering device (Ashford-Kent) for 2 min at a coating rate of 5 to 6 nm/min. The images were analyzed by ImageJ 1.48t software. Average fiber diameters were calculated based on 100 measurements made from images of different points of the samples.

Energy-dispersive X-ray spectroscopy (EDS) was performed using Phenom ProX SEM (Nanoscience Instruments). The specifications are 137 eV Mn Kα, and ZAF corrected. The accelerating voltage was 10 kV and samples were not coated before analysis.

Differential Scanning Calorimetry (DSC). A TA Instruments—Q200 DSC equipment was used for measuring the glass transition point of the fibers. About 2 to 5 mg of the sample was encapsulated in an aluminum pan and tested under a 50 mL/min flow of nitrogen. Moisture content of the samples was removed by heating them from 0 °C to 90 °C at a rate of 5 °C/min and keeping isothermal at 90 °C for 10 min. Then the samples were cooled to 0 °C. The softening point of O.L. is around 100 °C which overlap with the broad moisture evaporation peak. Therefore, samples were dried at 90 °C.

After removing the moisture, samples were heated from 0 to 180 °C (first heating cycle). After again cooling to 0 °C, the samples were heated to 200 °C (second heating cycle). The heating and cooling rates were 10 °C/min. Thermograms obtained from first and second heating cycles were analyzed.

Raman Spectroscopy. A Renishaw Raman imaging microscope was used to collect the spectra with a Near Infrared 780TF diode laser which had a wavelength of 785 nm. The 50× objective lens of the microscope was used to set the laser location on the samples. The instrument was calibrated by the silicone's Raman active vibration peak at 520 cm^{-1}. The spectra were collected between 500 and 2500 cm^{-1}. The laser power was set to 50% of 25 mW maximum output power. The scans were made using accumulation of two separate measurements of 20 s each. Three points of each sample were scanned.

Raman spectra were deconvoluted by Gaussian–Lorentzian curve fitting to three peaks.[45] The R^2 value for all the fittings was more than 0.97. The baseline was fitted by an exponential decay 2 function with a general equation of:

$$y = y_0 + A_1\, e^{-x/t_1} + A_2 e^{-x/t_2} \quad (1)$$

where y_0 = offset, A_1 and A_2 = amplitude, t_1 and t_2 = decay constant are equation parameters.

X-ray Diffraction (XRD). The carbonized fibers were grinded into fine powder by using mortar and pestle. Each sample was mounted on a glass fiber with vacuum grease. A SuperNova Agilent single-crystal diffractometer equipped with a microfocus CuKα (λ = 1.54184 Å) radiation source and Atlas CCD detector was used to study the samples at room temperature. X-ray diffraction images were collected from four different angular positions of the goniometer using ϕ scans to generate a 1D powder pattern within a 2θ range of 10 to 60°. The images were processed using CrysAlisPro software. Plots of the powder pattern were generated from the original images with a step of 0.02° in 2θ.

The interplanar spacing of crystalline planes was calculated using the Bragg's equation:

$$\lambda = 2\, d\, \sin\theta \quad (2)$$

where λ is the wavelength of the X-ray, d is the crystal plane spacing, and θ is diffraction angle.

Transmission Electron Microscopy (TEM). For sample preparation, carbonized fiber mats were put in distilled water and sonicated to separate and disperse the fibers in water. Then samples of dispersed material were taken by TEM grids with formvar/carbon film supports (Electron Microscopy Sciences). A field emission TEM from FEI Company (Tecnai G2 F20) was used for imaging the samples.

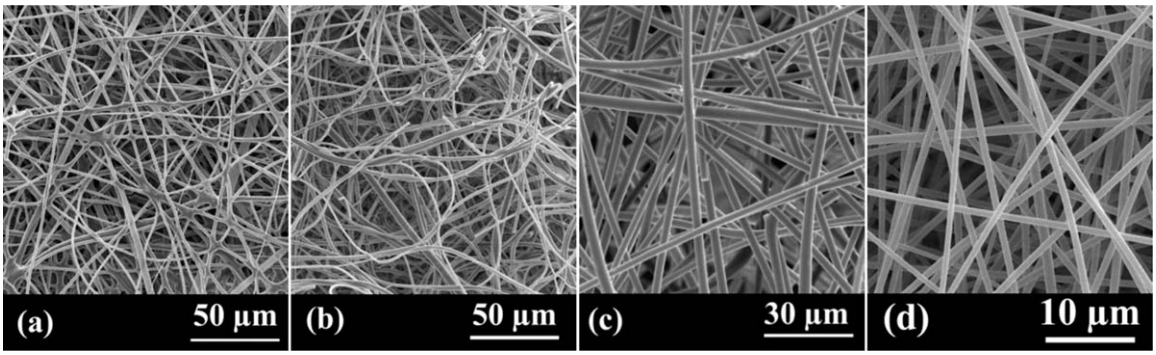

Figure 2. SEM images of the electrospun fibers from solutions of 7 wt % (O.L./PEO: 95/5) in aqueous sodium hydroxide (a) top surface of the fiber mat facing the needle, (b) bottom surface of the mat facing the collector, average diameter of fibers in (a and b) = 1.4 ± 0.3 μm, (c) O.L./PEO/aq NaOH fibers (spun from a mixed solution with 20 vol % ethanol) average diameter = 2.6 μm, (d) O.L./PEO/DMF electrospun fibers, average diameter = 0.8 ± 0.1 μm.

Results and Discussion

Electrospun O.L./PEO Fibers. In preliminary experiments, homogeneous solution of 7 wt % (O.L./PEO: 95/5) in aqueous sodium hydroxide was prepared without addition of ethanol. About 8 mL of the solution was electrospun with a feed rate of 0.6 mL/h (weight of the collected fiber was around 400 mg). Visual inspection of the collected fiber mat showed differences in the appearance of the two sides of the mat. The bottom side which was facing the collector looked fibrous and more flexible while the top side which was facing the needle looked like a brittle sheet. Low magnification SEM images of both sides were collected and compared. Images showed that the fibers on the top side of the mat were more interconnected [Figure 2(a)], while the bottom side was mostly made of free fibers [Figure 2(b)]. Since the fibers were spun from the same homogeneous solution, changes in solvent evaporation would be the cause of fibers interconnection on their contact points. At the beginning of the spinning, deposited fibers on the collector are separated and have enough time for drying before the next fibers fall on them. By passing time and increasing the amount of fibers, there is not enough time for drying and fibers merge together on their contact points. This situation became worse when the relative humidity of the spinning chamber increased to above 35% and temperature was below 30 °C. This effect reduces the yield of free fibers. One approach to reduce the interconnectivity of the electrospun fibers is to reduce the spinning time. This causes production of very thin fiber mats. The other approach is to increase the evaporation rate by addition of a volatile solvent like ethanol. Therefore, 20 vol % of ethanol was added to the solutions of 7 wt % (O.L./PEO: 95/5) before electrospinning of fibers for carbonization study. The fibers had less interconnection and were not merged together [Figure 2(c)]. They were more evenly spread on the collector foil and could be handled with less fiber breakage

Solution blends of O.L./PEO in DMF were also electrospun to compare the fibers spun from alkaline aqueous and organic solvent solutions. SEM image of the O.L./PEO/DMF electrospun fibers are shown in Figure 2(d). Compared with aqueous solutions, higher polymer concentration was required to be dissolved in DMF for successful spinning. The difference in required polymer concentration can be attributed to differences in polymer chain configuration and entanglements and also differences in surface tension of solvents.

Differential Scanning Calorimetry (DSC). Thermal transitions of electrospun lignin fibers and thermostabilized fibers were studied by DSC and compared with the O.L. powder. The DSC thermograms are shown in Figure 3.

First and second heating cycles of O.L. powder show a low softening temperature of 100 °C. The O.L./PEO/DMF fibers have a similar $T_g \approx 95$ °C in both heating cycles which as is expected is a close value to glass transition point of O.L. powder.

O.L./PEO/aq NaOH fibers show a different trend and do not have a detectable glass transition point in both cycles. In the thermogram of the first heating cycle, a broad endothermic peak around 140 °C is observed. The second heating cycle does not show any significant thermal event. T_g of lignin is inversely proportional to its hydrogen content which appears in C–H and O–H bonds.[46] Removal of glass transition point of O.L./PEO/aq NaOH fibers can be due to substitution of hydrogen in phenolic OH groups with sodium ions from alkaline solution. Dissolving O.L. in aqueous NaOH solution to prepare for the electrospinning causes structural changes in lignin which is reflected in thermal properties of the fibers. Appearance of the broad endothermic peak for these fibers can be attributed to re-orientation or some endothermic re-organization of the polymer chains in these fibers. During electrospinning, networks of entangled polymer chains are extended along the electrical force direction. When the solvent evaporates and the fibers solidify, the chains freeze into their extended state.[47] This endotherm has been reported to be a sign of conformational rearrangement of molecules from the oriented glassy to the isotropic rubbery state.[47,48] The same endothermic peak which appeared for as-spun fibers is also observed for thermostabilized fibers. The slow heating rate during thermostabilization, can be one of the reasons that even after thermostabilization, the fibers show the endothermic peak in DSC.

After completion of each DSC experiment, the sample was examined. Lignin powder sample had turned into a solid piece of dark material due to softening and merging of the particles. The same happened to O.L./PEO/DMF fibers but O.L./PEO/aq

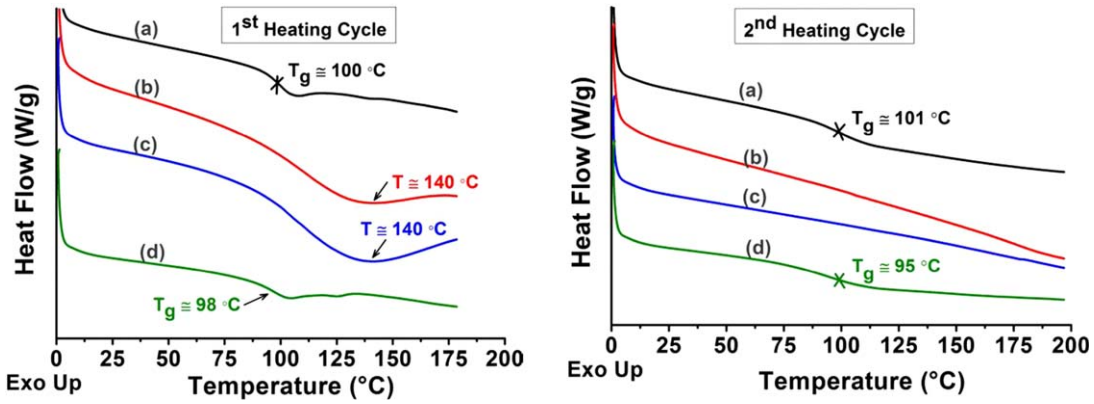

Figure 3. DSC thermograms of first and second heating cycles of (a) O.L. powder, (b) electrospun fibers of O.L./PEO/aq NaOH, (c) thermostabilized fibers of (b), (d) electrospun fibers of O.L./PEO/DMF. [Color figure can be viewed in the online issue, which is available at wileyonlinelibrary.com.]

NaOH fibers and thermostabilized fibers remained unchanged and preserved their fibrous network after DSC cycles.

Thermostabilization and Carbonization of the Fibers. The O.L./PEO/aq NaOH fibers were thermostabilized at 250 °C for 2 h and a heating rate of 0.5 °C/min. To confirm resistance of the fibers to melting, they were subsequently carbonized at 1000 °C with a heating rate of 5 °C/min. SEM images [Figure 4(a)] showed the fibers were carbonized without considerable melting or fusion of the fibers.

Since the DSC results of O.L./PEO/aq NaOH fibers did not show a noticeable glass transition point, carbonization of the as-spun fibers without passing the thermostabilization step was also tested. SEM images of the fibers showed successful carbonization without melting or fusion of the fibers [Figure 4(b)]. The average fiber diameter was close to the carbonized fibers which passed the thermostabilization. Hu and Hsieh[35] reported direct carbonization without thermostabilization of (alkali lignin/PEO: 9/1 w/w) blend fibers electrospun from aqueous solutions with and without addition of NaOH or KOH. They carbonized the fibers at both 600 and 850 °C with a heating rate of 10 °C/min.

In experiments designed for statistical analysis of the carbonization parameters, the O.L./PEO/aq NaOH fibers were passed through both of the thermostabilization and carbonization steps

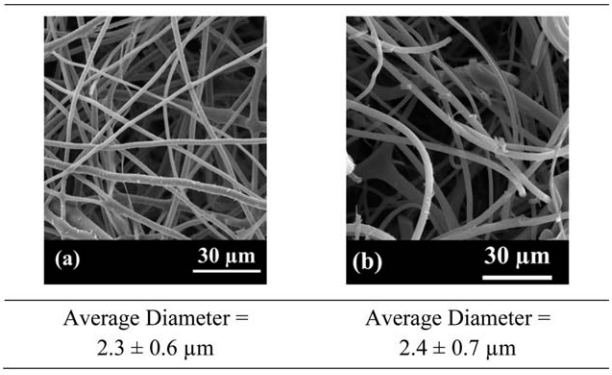

Figure 4. SEM images of carbonized O.L./PEO/aq NaOH fibers, (a) carbonized fibers after thermostabilization, (b) carbonized fibers without thermostabilization.

to have a comparable thermal history with the carbonized fibers reported in the literature. It is also observed from DSC results that some chain realignment happens when the fibers are first heated to 200 °C. This may change the microstructure of the carbonized fibers. Studies which reported effects of carbonization parameters had thermostabilized the fibers at 200, 250, 300 °C, for 1, 2, 36 h.[40–42] In this study, an intermediate thermostabilization temperature and time of 250 °C and 2 h were selected.

When O.L./PEO/DMF fibers [Figure 5(a)] were heated at the same thermostabilization conditions as O.L./PEO/aq NaOH fibers, they melted and left a black solid residue [Figure 5(b)]. Then the following program was applied to thermostabilize the fibers: heating to 90 °C with a rate of 0.5 °C/min then 2 h isothermal, stepwise 10 °C increase in temperature at the same rate of 0.5 °C/min and 2 h isothermal up to 200 °C. The same procedure was also repeated with a heating rate of 0.1 °C/min. After both attempts, the fibers were shrunk and melted together as it is shown in Figure 5(b). It is in agreement with behavior of organosolv lignin which requires thermostabilization at very slow heating rate and long processing times.[20,40,49] It highlights the importance of taking advantage of an environmentally friendly aqueous alkali hydroxide solution to dissolve lignin for electrospinning of precursor fibers.

Morphologies of Carbonized Electrospun O.L./PEO/aq NaOH Fibers. SEM images of electrospun O.L./PEO fibers and thermally treated samples prepared according to the design of experiments (Table II) are shown in Figure 6. Average diameter of nine batches of electrospun fibers, made for the nine carbonization experiments, was between 2.2 ± 0.6 and 3.1 ± 0.7 µm. The fibers spun from aqueous solutions usually have larger diameters compared with fibers spun from organic solvents such as DMF.[26,35,36] During thermostabilization, low molecular weight volatile material and weak groups on the polymer backbone leave the fibers resulting in weight reduction of the material. Average yield of thermostabilization was 83 ± 3 wt %. Average diameter of the thermostabilized fibers was 2.6 ± 0.6 µm. Thermostabilization did not have significant effect on reduction of fiber diameters. Lallave *et al.*[34] also reported no change in diameter of Alcell lignin fibers after thermostabilization.

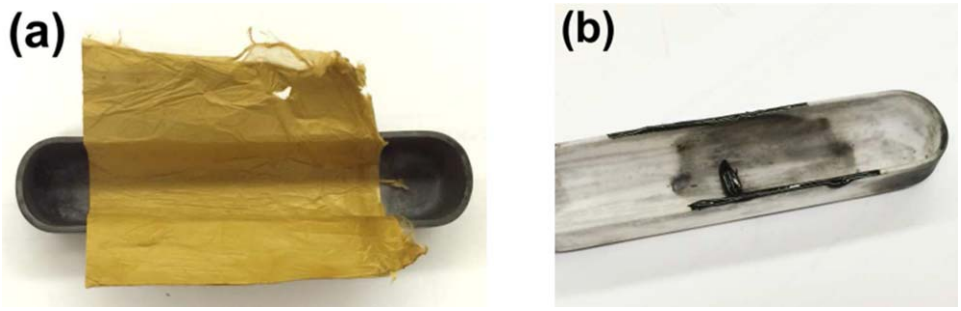

Figure 5. Electrospun O.L./PEO/DMF fibers, (a) as-spun fibers, (b) black solid residue after thermal process at 200 °C. [Color figure can be viewed in the online issue, which is available at wileyonlinelibrary.com.]

The average percentage of diameter reduction for the nine carbonized samples was about 27.7 ± 6.4%. This result is in agreement with results obtained for fibers made from aqueous solution of alkali lignin/PVA. Blend fibers with 30, 50, and 70 wt % of lignin had about 28 ± 4% reductions in diameter.[22] Lallave *et al.*[34] produced both filled and hollow carbon fibers from Alcell lignin solutions in ethanol. Diameter of their fibers was in the range of 400 nm to 2 μm which after carbonization reduced to around 200 nm. The diameter reduction is attributed to the mass loss due to removal of elements such as hydrogen and oxygen (and sulfur for kraft lignins).[22]

After carbonization, the fibers preserved their fibrous structure without major fusion or merging. Average diameter of each sample after carbonization is reported in Table III.

The fibers carbonized at 800 °C had a rough surface compared with the ones carbonized at 1100 °C. EDS analysis of the fiber surface showed a higher percentage of inorganic material on the rough surfaces. The inorganic material was mainly from the sodium hydroxide in the spinning solution which was carried and remained with fibers when the solvent evaporated; and also ash content of the lignin. When the fibers were carbonized at low temperatures the inorganic material did not completely evaporate from the fibers and solidified and recrystallized on the surface during cooling the samples. The fibers carbonized at 1100 °C, did not have rough surfaces but some shallow pores were visible on some areas of the fibers. Gao *et al.*[43] also observed the similar spherical roughness on the surface of electrospun lignin fibers which contained Pd, Pt, or a combination of these metal particles.

Effects of the three thermal treatment parameters on the carbonized fiber diameter were evaluated by statistical analysis of the diameter of samples made according to design of experiments. Figure 7 is the Pareto chart of standardized effects for diameter. It shows that carbonization time followed by heating rate have the highest significant effect on the diameter. Interaction of the three variables is the next significant effect. Two variable interactions and temperature are the nonsignificant parameters.

Main effects and interaction plots are shown in Figure 8. Increasing the heating rate and carbonization time reduces the diameter. Temperature alone did not show a significant effect but it shows the effect by interaction with other parameters. Heating rate and temperature showed the highest interaction. With increasing the heating rate, the highest temperature causes more reduction in diameter. Time and heating rate, both, reduce the diameter with more reduction happening for higher times and higher heating rates. Time and temperature has the smallest amount of interaction.

Raman Spectroscopy of the Fibers. Raman spectra of carbonized fibers showed two peaks associated with sp^2 and sp^3 hybridizations of carbon. The peaks are located around 1300 to 1320 and 1580 to 1600 cm^{-1} corresponding to sp^3 (D band) and sp^2 (G band) hybridizations, respectively.[50,51] The Raman spectrum of each sample was deconvoluted to three peaks; two Lorentzian peaks in the ranges of 1580 to 1600 cm^{-1} and 1297 to 1320 cm^{-1} for the G and D bands, and a Gaussian peak in the range of 1480 to 1590 cm^{-1} between the D and G peaks. The last peak is to improve the adjusted R^2 of the fitted peaks.[52] The R^2 value for the fits was more than 0.97 for all the measurements. The peak deconvolution for one of the carbonized fiber samples are shown in Figure 9.

D band is an indication of polycrystalline graphite. It represents a material with turbostratic carbon structure in which the carbon atoms are disordered around the graphite sheets. The G band presents carbon structure in a single crystal of graphite.[53] Ratio of intensity of D band to G band ($R = I_D/I_G$) indicates the degree of graphitization and ordered structure. The R value is also used to calculate the graphitic mole fraction (x_G) and crystallite size [L_a (nm)] according to the following equations[54,55]:

$$\text{Graphitic mole fraction}: \quad x_G = \frac{I_G}{I_D + I_G} = \frac{1}{1+R} \tag{3}$$

$$\text{Crystallite size}: \quad L_a = \left(2.4 \times 10^{-10}\right) \lambda^4 \, (R)^{-1} \tag{4}$$

In eq. (4), λ is the wavelength of the incident laser (785 nm). Characteristic peak information is summarized in Table IV and their statistical analyses are discussed in the subsequent sections.

Effect of Thermal Parameters on D and G Band Positions. Many factors can affect the positions of Raman peaks of carbonaceous materials, such as nitrogen doping on the fiber surface, numbers of layers, defects, strains, substrate, etc. Addition of defects causes a change in vibration energy levels.[24,56]

According to the Pareto chart in Figure 10(a), temperature and time have significant effect on the center point of D band. With increasing these two parameters the band position shifted to a

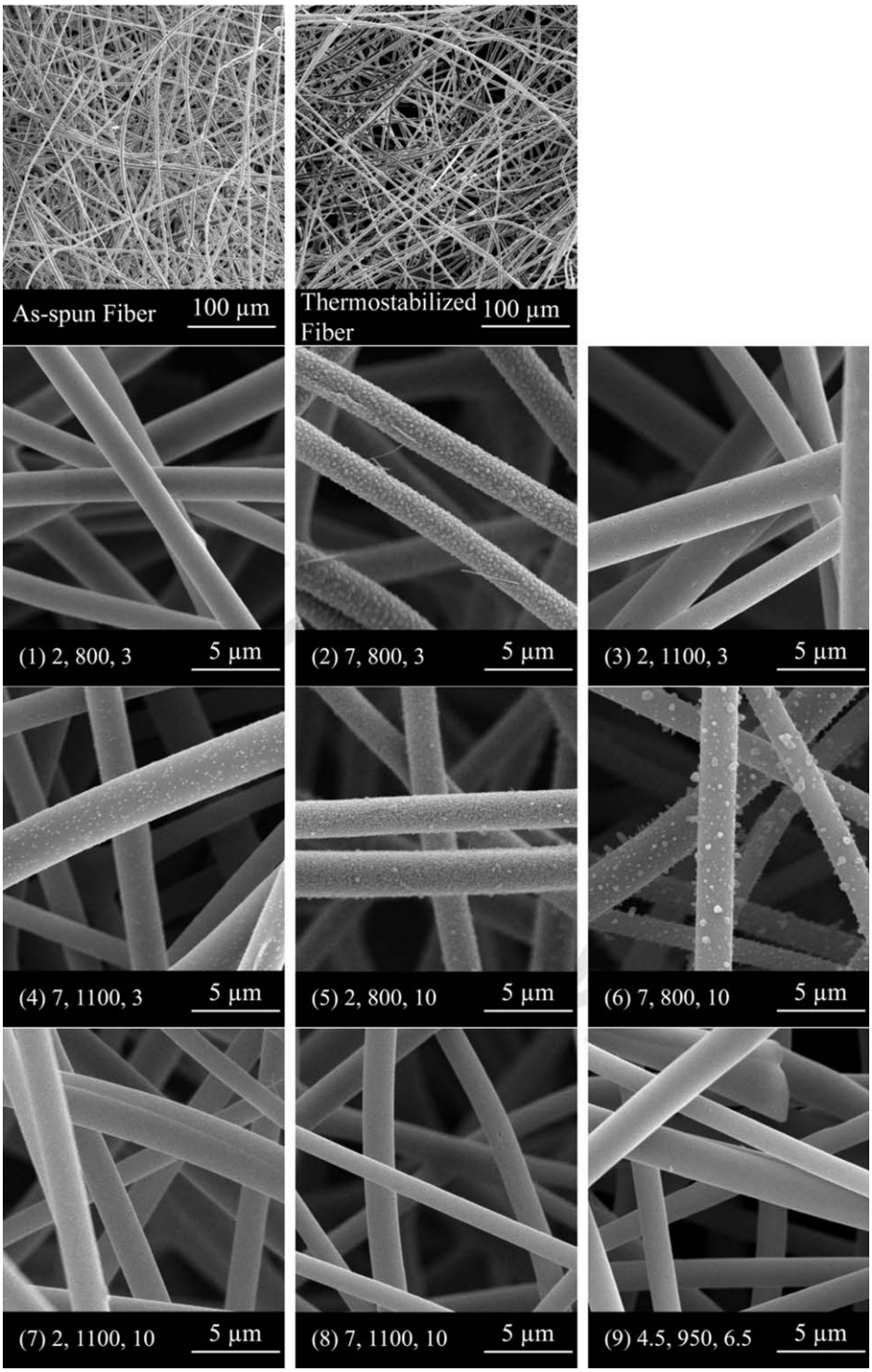

Figure 6. SEM images of as-spun, thermostabilized and carbonized O.L./PEO/aq NaOH fibers. Numbers under each image are: (sample number according to Table II) heating rate (°C/min), carbonization temperature (°C), time (h).

lower value [Figure 11(a)]. Interaction terms are the next important parameters and heating rate is the last one [Figure 10(a)]. For samples prepared at higher temperatures or longer times, the changes in heating rate do not change the D band position and the position stays at lower Raman shifts compared with lower times or temperatures [Figure 11(c)].

For center point of the G band [Figure 10(b)], carbonization temperature, heating rate, and all the two-by-two interactions are significant parameters. Increasing the temperature shifted the band position to higher values, which is opposite to the effect on D band position [Figure 11(a,b)]. The interaction plots show that when the fibers are carbonized for long hours,

Table III. Average Diameter of Thermostabilized Fibers, Carbonized Fibers, and Carbonization Yield

No.	Thermostab. fiber average dia. (μm)	Carbonized fiber, average dia. (μm)	Carbonization yield (%)
1	2.8 ± 0.5	2.2 ± 0.5	42.6
2	2.6 ± 0.7	2.2 ± 0.5	45.7
3	2.7 ± 0.6	2.1 ± 0.4	—
4	2.8 ± 0.5	2.0 ± 0.4	32.4
5	2.5 ± 0.5	2.1 ± 0.4	40.3
6	2.6 ± 0.6	1.7 ± 0.4	44.2
7	2.3 ± 0.5	1.6 ± 0.4	32.5
8	2.5 ± 0.5	1.8 ± 0.5	40.4
9	2.8 ± 0.5	1.9 ± 0.4	27.6

Sample numbers are in the same order as Table II. Yield of sample 3 was not available.

the heating rate and temperature do not affect position of the G band [Figure 11(d)].

Effect of Thermal Parameters on D and G Band Full Width at Half Maximum (FWHM). FWHM of the bands is a measure of degree of graphitization. Narrower peaks show more ordered structures.[57]

Carbonization temperature has significant effect on reducing the FWHM of D band [Figures 12(a) and 13(a)]. Heating rate and time are not significant variables but their increase widens the band [Figure 13(a)].

Increasing the carbonization time and temperature significantly reduces FWHM of G band [Figure 13(b)]. Interaction between these two variables is also a significant factor. At shorter carbonization time, increasing the temperature narrows the G band, while for longer times, increasing the temperature has the opposite effect [Figure 13(d)].

Effect of Thermal Parameters on *R* Value. *R* value was calculated from the ratio of height of deconvoluted peaks. This value is a measure of the ordered structure and is inversely proportional to the crystalline size of graphite sections. With increasing the *R* ratio, the crystalline size decreases. *R* values more than one show the presence of disordered structure is more dominant compared with graphitic structure.

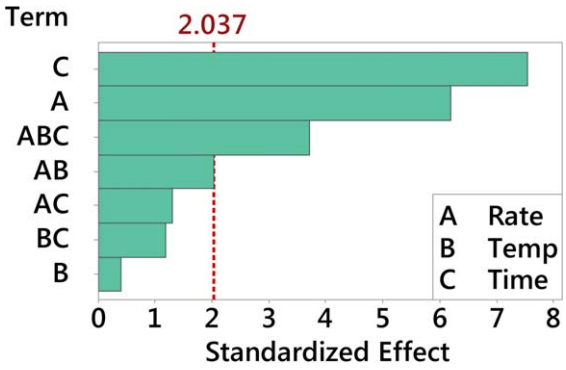

Figure 7. Pareto chart of standardized effect. Response is diameter of carbonized fibers, α = 0.05. [Color figure can be viewed in the online issue, which is available at wileyonlinelibrary.com.]

Results of the statistical analysis showed that the three parameters in the selected range did not have significant effect on the *R* value of the carbonized fibers. The parameters with highest influence were interaction between heating rate and temperature, temperature, and time (Figure 14).

The main effects and interaction plots show that increasing the carbonization temperature reduces the *R* value (Figure 15). At higher temperature more organized graphitic structure is formed. Effect of increasing the carbonization time on the *R* value is opposite to the temperature. At longer times the *R* value increases which means increasing the intensity of D band. Interaction plots show that *R* value can be decreased at longer times by increasing the heating rate or increasing the temperature [Figure 15(b)].

The effect of heating rate on the *R* value depends on the temperature. For higher temperatures, increasing the heating rate increases the *R* value but at lower temperatures, increasing the heating rate causes formation of more graphitic structure and the *R* value decreases [Figure 15(b)].

Effect of Thermal Parameters on Graphitic Mole Fraction (x_G) and Crystallite Size (L_a). Calculated values for x_G are reported in Table IV and used for statistical analysis. The parameter levels tested in this study did not have significant

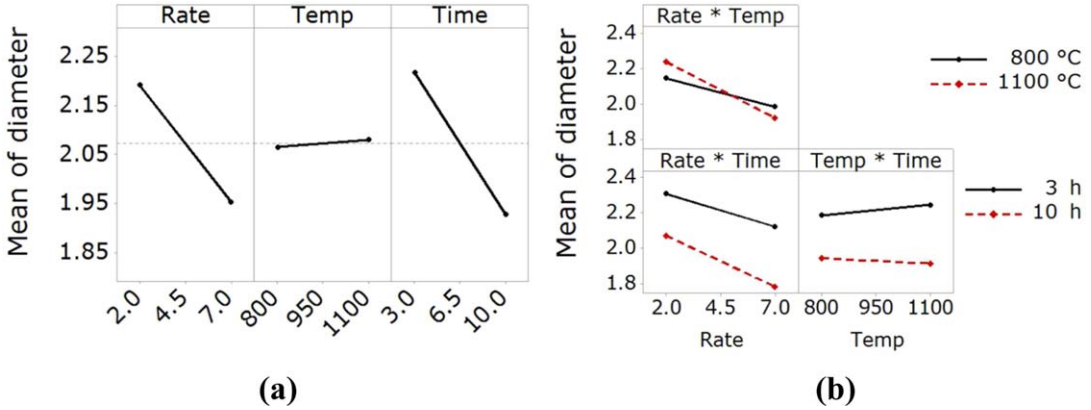

Figure 8. (a) Main effects and (b) interaction plots for diameter of carbonized fibers. [Color figure can be viewed in the online issue, which is available at wileyonlinelibrary.com.]

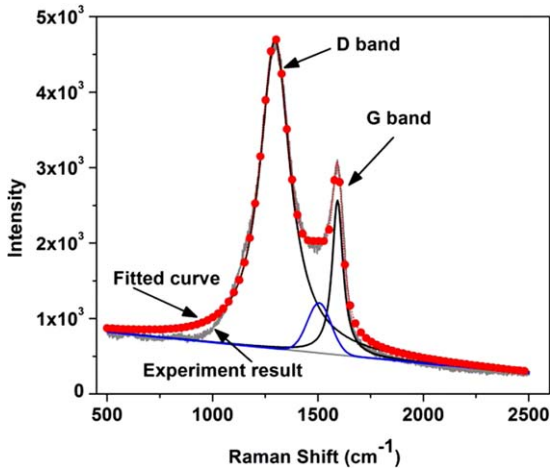

Figure 9. Deconvolution of Raman spectrum of a carbonized Fiber. Red dotted line is the fitted curve after peak deconvolution. [Color figure can be viewed in the online issue, which is available at wileyonlinelibrary.com.]

effect on x_G of the carbonized fibers [Figure 16(a)]. The order of the important variables is similar to the order for the R value. The main effect plots [Figure 17(a)] show x_G increases by increasing the temperature and heating rate. Longer carbonization time reduces the graphitic mole fraction. Among interactions, the one between heating rate and temperature has the highest influence [Figure 17(c)]. Selecting a higher heating rate to reach the high temperature level reduces the x_G but for lower temperature, it has an opposite effect.

Graphitic crystallite size (L_a) is inversely proportional to the R value. Therefore, same as R value, there is no significant variable on Pareto chart of the carbonized fibers [Figure 16(b)]. Interaction between time and heating rate has the most influence on the response of L_a. Increasing the heating rate to reach the lower carbonization temperature, increases the L_a but for higher carbonization temperature, heating rate has the opposite effect [Figure 17(d)]. Carbonization time is the next important variable in reducing the L_a. Increasing the temperature or time increases the size of crystallites.

Ruiz-Rosas *et al.*[40] reported carbonization of electrospun fibers from Alcell lignin with and without platinum as filler. The carbonization heating rate was 10 °C/min and they tested carbonization at 600, 800, 900, and 1000 °C. They observed narrowing of D and G band which is also predicted in Figure 13. They also observed an increase in the G band intensity with increasing the temperature, which is equivalent to reduction of R value (Figure 15). The

Table IV. Characteristic Peak Information of Deconvoluted Raman Spectra of Carbonized Fibers

No.	D band center position (cm^{-1})	G band center position (cm^{-1})	R ratio	D band FWHM[a]	G band FWHM	x_G	L_a
1	1308.6 ± 4.7	1594.1 ± 2.5	2.4 ± 0.4	212.7 ± 3.5	95.1 ± 11.3	0.296 ± 0.032	38.5 ± 5.7
2	1320.2 ± 11.9	1584.7 ± 7	2.2 ± 0.9	200.5 ± 53.1	96.9 ± 20.7	0.336 ± 0.088	47.6 ± 17.5
3	1304.1 ± 1.1	1600.0 ± 0.4	2.0 ± 0.1	178.7 ± 3.6	73.5 ± 3.4	0.335 ± 0.006	45.9 ± 1.2
4	1301.4 ± 1.0	1594.4 ± 2.5	2.3 ± 0.4	190.9 ± 6.6	65.4 ± 5.4	0.306 ± 0.029	40.3 ± 5.4
5	1307.5 ± 4.6	1594.1 ± 1.6	3.0 ± 0.6	219.9 ± 13.2	55.0 ± 0.8	0.257 ± 0.035	31.7 ± 5.9
6	1306.3 ± 3.3	1589.0 ± 0.9	2.3 ± 0.1	223.7 ± 5.6	74.6 ± 4.3	0.298 ± 0.006	38.7 ± 1.1
7	1300.5 ± 3.3	1591.1 ± 2.3	2.2 ± 0.1	195.6 ± 2.1	72.2 ± 7.7	0.307 ± 0.005	40.5 ± 1.0
8	1301.1 ± 1.3	1594.3 ± 1.0	2.3 ± 0.3	200.9 ± 4.9	72.5 ± 2.7	0.307 ± 0.028	40.5 ± 5.2
9	1297.8 ± 0.4	1593.9 ± 4.2	2.2 ± 0.1	196.3 ± 9.4	59.6 ± 2.6	0.310 ± 0.008	40.9 ± 1.6

Sample numbers are in the same order as Table II. Data are average of three measurements.
[a] Full width at half maximum of the peak.

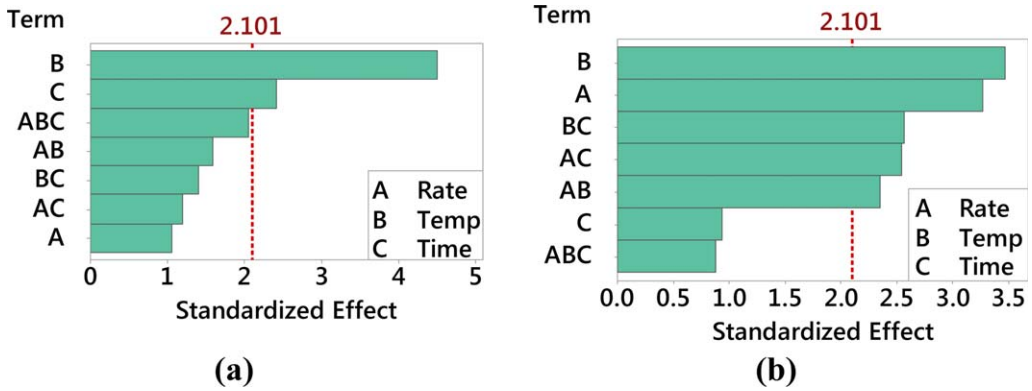

Figure 10. Pareto chart of standardized effect. Response is position of Raman bands for carbonized fibers, (a) position of D band, (b) position of G band. [Color figure can be viewed in the online issue, which is available at wileyonlinelibrary.com.]

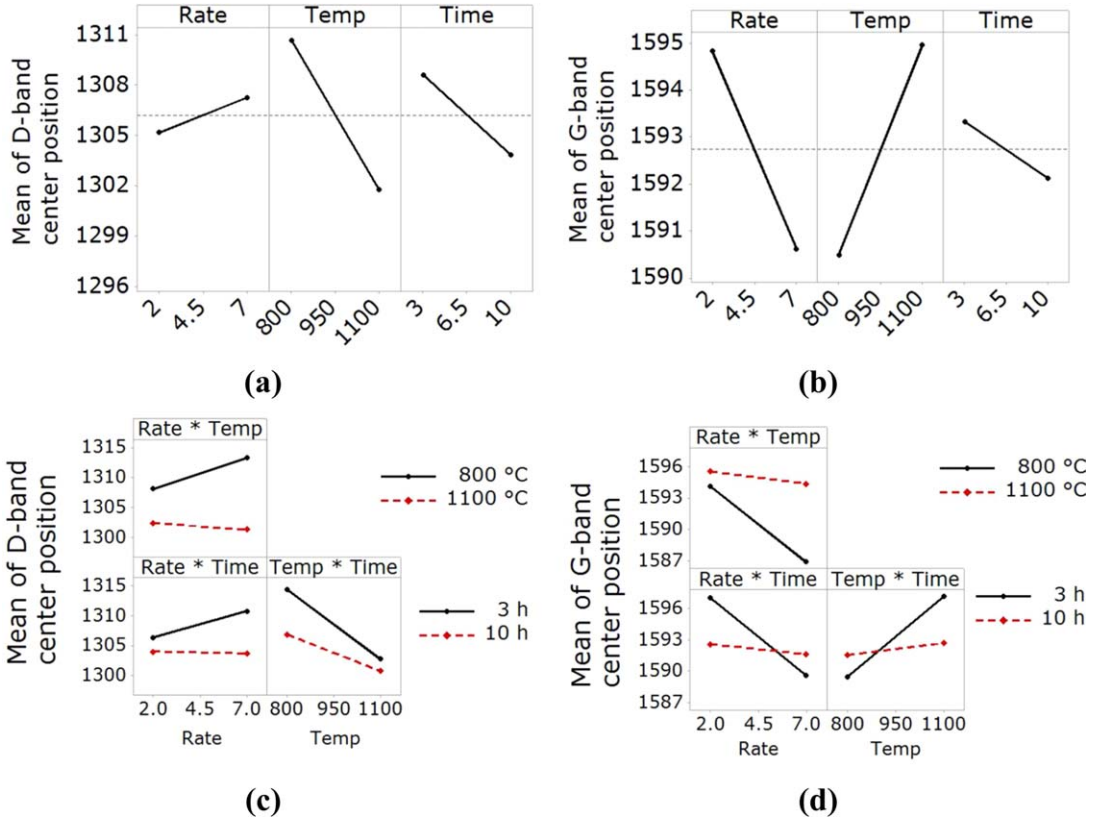

Figure 11. Main effect and interaction plots for position of Raman bands for carbonized fibers. Main effect plots for center position of (a) D band, (b) G band; interaction plots for center position of (c) D band, (d) G band. [Color figure can be viewed in the online issue, which is available at wileyonlinelibrary.com.]

results showed dispersion of platinum slightly hindered the graphitization of the fibers. It was observed by broadening of D band and reduction in G band intensity.

Dallmeyer *et al.*[42] reported carbonization of electrospun lignin fibers produced from a blend of PEO with solvent fractionated kraft lignin. Two ends of the strips of fibers were clamped during carbonization experiment. The fibers were thermostabilized and carbonized by heating to 250 °C at a rate of 20 °C/min followed by heating to 600, 800, or 1000 °C at a rate of 10 °C/min and 1 h isothermal. By increasing temperature, the *R* value, FWHM, and Raman shift of G band increased while FWHM of D band decreased and position of D band remained the same. The increase in *R* values for carbonized lignin fibers can be explained by the interaction curves. The main effect plots shown in Figure 15(a) suggest that with increasing the temperature, the *R* value decreases. However, Figure 14(a) shows interaction between heating rate and temperature has more effect than temperature alone. Figure 15(b) shows the effect of interactions between heating rate and temperature. The two curves cross each other just before 7 °C/min. If they are extrapolated to higher rates, it is observed that experiments at higher temperatures result in higher *R* values than lower temperatures. For

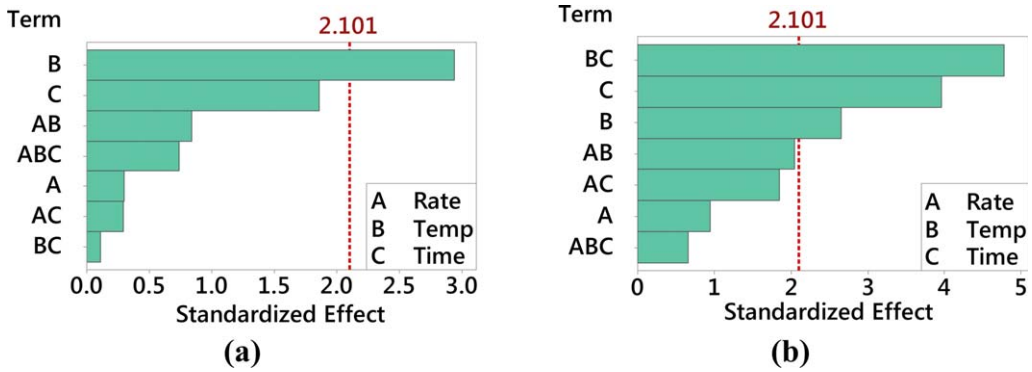

Figure 12. Pareto chart of standardized effect. Response is FWHM of (a) D band, (b) G band. [Color figure can be viewed in the online issue, which is available at wileyonlinelibrary.com.]

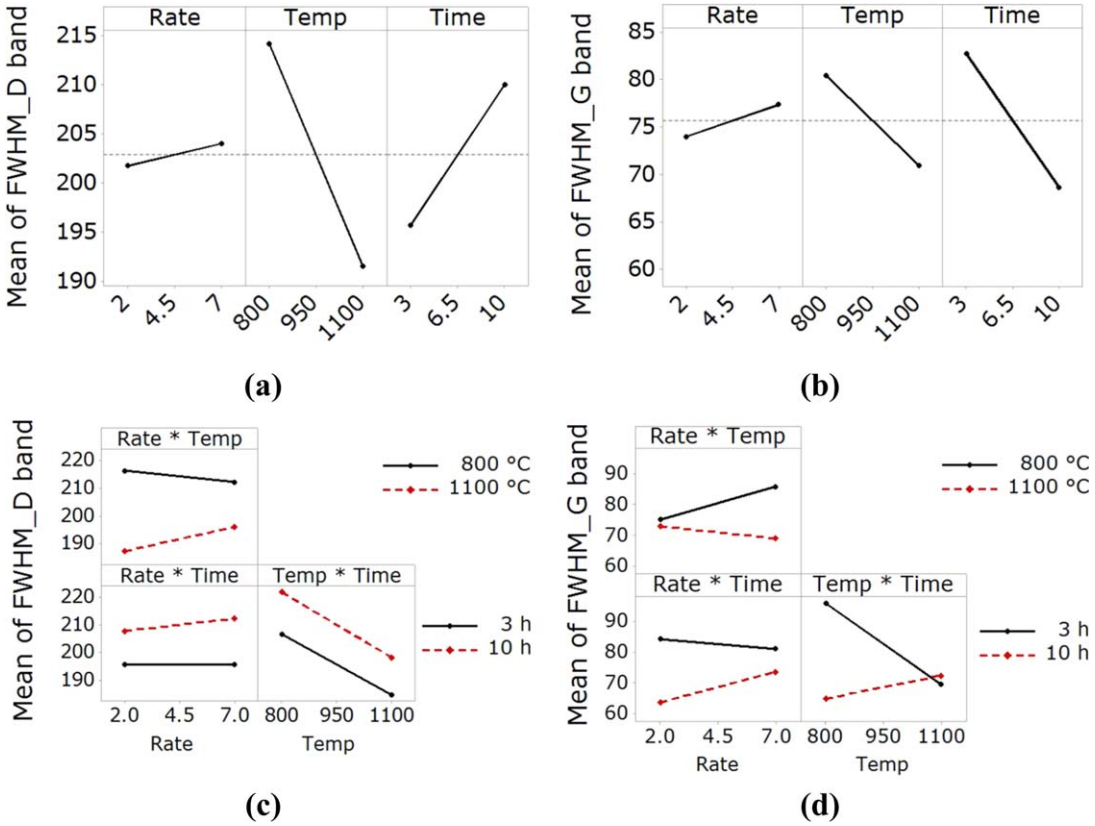

Figure 13. Main effect plots for FWHM of (a) D band, (b) G band; interaction plots for FWHM of (c) D band, (d) G band. [Color figure can be viewed in the online issue, which is available at wileyonlinelibrary.com.]

FWHM of D band, temperature is the significant variable. The results showed its reduction for lignin fibers with increasing the temperature, which is consistent with Figure 13(a). The increase in FWHM of G band for lignin is not consistent with the effects of significant parameters. Only increasing the heating rate increases the FWHM [Figure 13(b)]. The observed increase in FWHM for carbonized lignin fibers suggests that it may be possible that at high heating rates, this effect becomes more prominent. For position of D and G bands, temperature is the significant parameter for D band [Figure 10(a)]. Increase in temperature reduces the D band Raman shift. Position of G band is affected significantly by temperature [Figure 10(b)]. In the studied range, by increasing the temperature, the G band position shifts to higher frequency [Figure 11(b)].

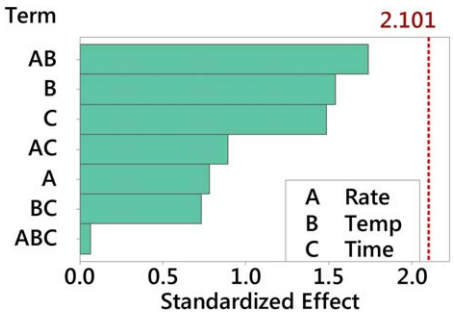

Figure 14. Pareto chart of standardized effect. Response is *R* value. [Color figure can be viewed in the online issue, which is available at wileyonlinelibrary.com.]

Schreiber *et al.*[41] studied the carbonization of iodine treated and non-treated electrospun blend fibers of hardwood organosolv lignin (Lignol Innovations, Ltd.) and cellulose acetate (CA) with two different lignin to CA blend ratios of 2/1 and 4/1. They could have successful carbonization of fibers at a heating rate of 2 °C/min to 800 or 1000 °C and carbonization time of 1 h. This is close to conditions of samples No. 1 and No. 3 of this report. They observed similar D band positions especially at high lignin contents to this report. However, for the G band, they observed lower Raman shifts at the maximum point of the peak. They observed a higher *R* ratio, which shows more disordered structure. They also observed a lower FWHM for D band, smaller crystalline size (L_a), and lower graphitic mole fraction (x_G). These effects could be due to addition of a second polymer or less molecular orientation during the electrospinning of the fibers.

X-ray Diffraction Analysis. The X-ray patterns of the carbonized fibers are shown in Figure 18. All the graphs have a broad peak spanning in the range of 15 to 33° with a maximum at 2θ ≈ 23° which corresponds to (002) crystallographic plane of graphite. The wide range of the peak suggests the crystallites have a small size and they have a low degree of order.[22,27] Another smaller peak is also visible with a maximum at 2θ ≈ 43° which is related to diffraction from (100) planes.[58] The

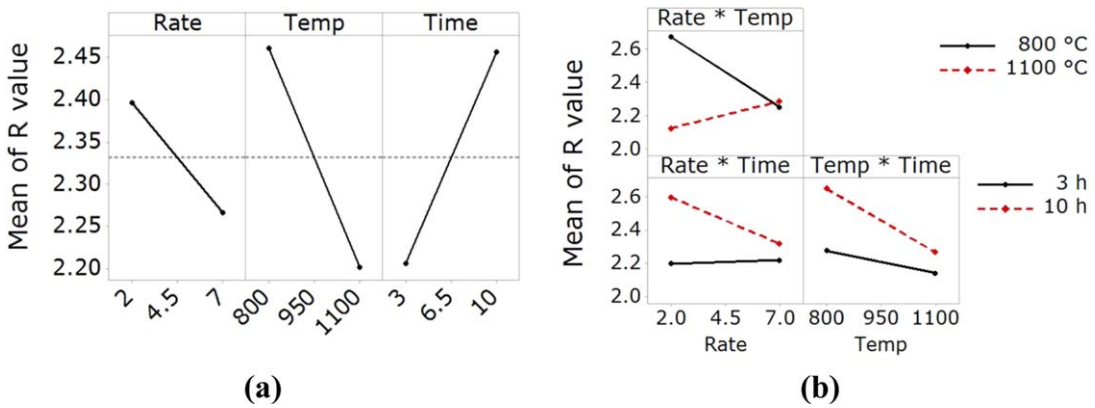

Figure 15. (a) Main effect plots for *R* value of carbonized fibers, (b) interaction plots for *R* value of carbonized fibers. [Color figure can be viewed in the online issue, which is available at wileyonlinelibrary.com.]

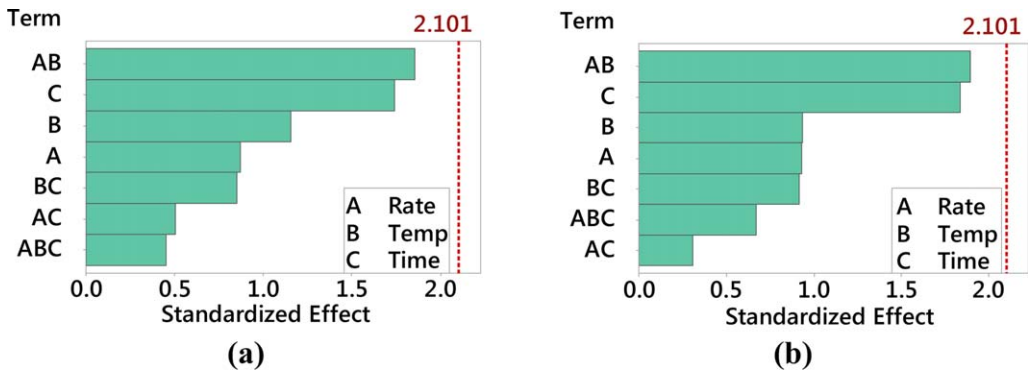

Figure 16. Pareto chart of standardized effect. Response is (a) graphitic mole fraction, (b) crystallite size. [Color figure can be viewed in the online issue, which is available at wileyonlinelibrary.com.]

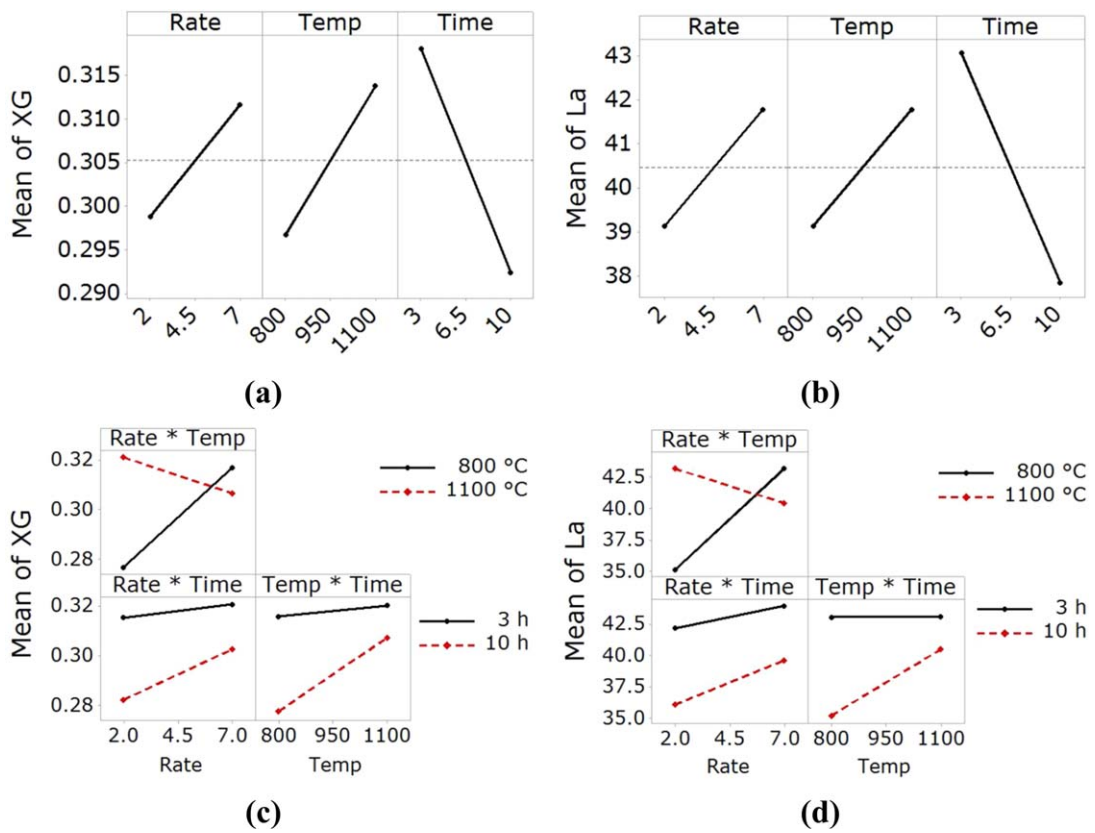

Figure 17. Main effect plots for (a) graphitic mole fraction, (b) crystallite size of carbonized fibers. Interaction plots for (c) graphitic mole fraction, (d) crystallite size of carbonized fibers. [Color figure can be viewed in the online issue, which is available at wileyonlinelibrary.com.]

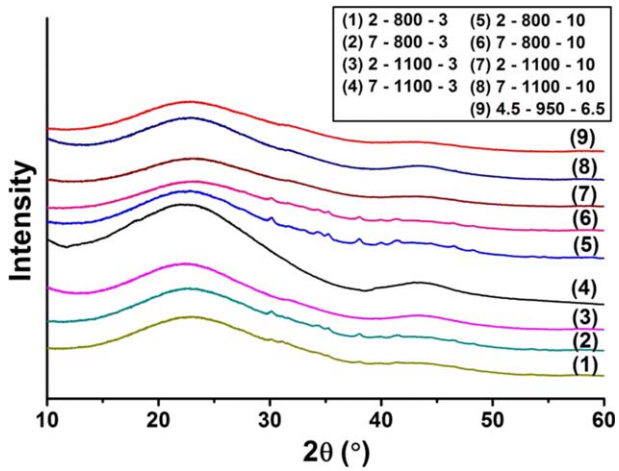

Figure 18. XRD graphs of carbonized fibers. The numbers on the graphs are the sample numbers according to Table II. The numbers in the legend are heating rate (°C/min) – temperature (°C) – time (h). [Color figure can be viewed in the online issue, which is available at wileyonlinelibrary.com.]

average interplanar spacing, d(002), calculated from the Bragg equation [eq. (2)] for the carbonized fibers was between 0.379 and 0.390 nm. The interlayer spacing indicates the degree of packing of the crystal structure. Its reduction can be an indication of more porous structure and lower density.[22] Lai *et al.*[22] calculated the d(002) spacing for carbonized fibers from blends of alkali lignin and PVA. The fibers were heated to 1200 °C at a rate of 5 °C/min and kept for 1 h to carbonize. The interplanar spacing increased by increasing the lignin content in the precursor fibers and reached to 0.418 nm for carbonized fibers of lignin/PVA:70/30.

The results of statistical analysis of d(002) spacing are shown in Figure 19. It shows that interaction between all the three parameters has the significant effect on the interlayer spacing. Among all the parameters, carbonization time has the highest effect on the packing of the layers. The interaction plots show that for long carbonization times, heating rate and temperature do not have effect on the d spacing but at shorter times, higher heating rate and higher temperatures create the same effect.

TEM Analysis. The carbonized fibers were dispersed in water and sonicated to break them in smaller and thinner pieces which could be analyzed by TEM. Images show that each particle is made of multiple layers and circular structures are observed on the edges and also inside the bulk of the material (Figure 20). Lignin is described to have self-similarity and is described as a fractal object.[59] It may explain the regular circular patterns in the fibers. Thinner sections of the fibers also demonstrate high porosity of the material.

Samples 2, 6, 7, 8, 9 (Figure 20) which were carbonized at higher heating rate and longer times demonstrate aggregates of parallel crystal lines which are stacks of graphene sheets. By increasing the carbonization temperature, the lines become longer which is an indication of increase in graphene crystal size. The aggregates are not oriented in a preferred direction, especially in fibers carbonized at lower temperature. Examination of

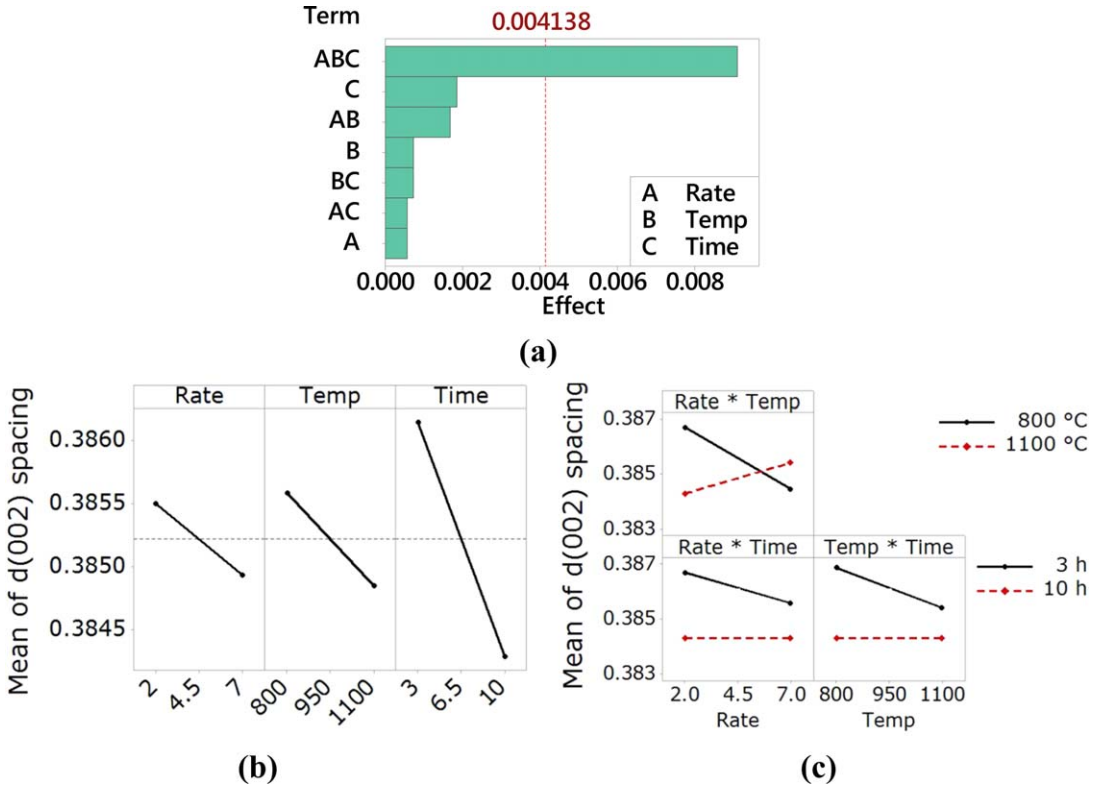

Figure 19. Statistical analysis results for d(002) spacing (a) pareto chart of standardized effect, (b) main effect plots, (c) interaction plots. [Color figure can be viewed in the online issue, which is available at wileyonlinelibrary.com.]

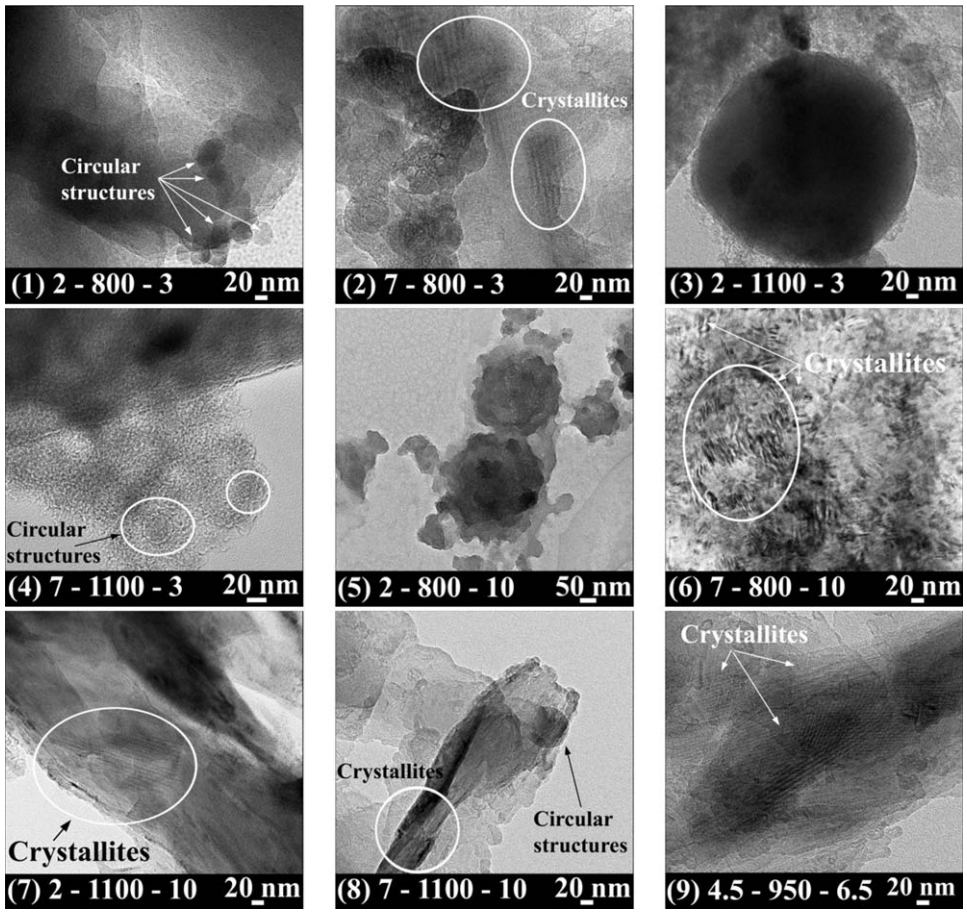

Figure 20. TEM images of the carbonized fibers. The numbers under each image are: (sample no.) carbonization heating rate (°C/min) – temperature (°C) – time (h). Samples of regions with crystallites and also circular structures are marked on the images.

multiple TEM images of one sample showed existence of both disordered and ordered domains in samples 2, 6, 7, 8, 9. Similar graphitic structures were observed in TEM images of electrospun PAN fibers carbonized at 1100 °C[60] or the electrospun PAN fibers carbonized at 1000 °C and graphitized at 2200 °C.[61] For most of the carbonized electrospun lignin blend fibers, formation of a porous and turbostratic structure is reported.[22,24] Johnson *et al.*[62] examined the structure of commercial carbon fibers produced from dry-spun lignin/PVA precursor fibers carbonized at 1500 and 2000 °C. They reported formation of circular inclusions in fibers carbonized at 1500 °C. The areas in the wall of circular inclusions had more lattice order compared with the rest part of the fiber. The highly ordered regions of graphitic layers appeared when the fibers were treated at 2000 °C.

CONCLUSIONS

Lignin-based fibers were electrospun from a blend of organosolv lignin/PEO with 95/5 wt/wt ratio in a mixture of aqueous NaOH and ethanol (80/20 v/v). Although organosolv lignin powder had a low glass transition point (~100 °C) leading to fusion upon heating, dissolving lignin in alkaline aqueous solution improved the thermal stability of the material. The lignin-based fibers did not show a glass transition point and remained unchanged after heating. It enabled direct carbonization of the fibers at 1000 °C and a heating rate of 5 °C/min without thermostabilization. In comparison, fibers with the same composition electrospun from solution of the lignin/PEO blend in DMF exhibited similar T_g to lignin powder. These fibers could not withstand thermostabilization at a heating rate of 0.1 °C/min and fused together.

Effects of different levels of carbonization parameters on the microstructure of carbonized electrospun lignin/PEO fibers were statistically analyzed by using a two-level factorial design of experiments. The studied carbonization parameters were temperature, isothermal time at maximum temperature, and heating rate.

Average carbonization yield was about 38%. Average diameter of as-spun fibers was 2.6 ± 0.6 μm and reduced to ~2 μm after carbonization. Statistical analysis showed heating rate and time have significant effects on the diameter of the carbonized fibers. Characteristics of deconvoluted Raman spectra showed that temperature is the significant variable for most of the properties followed by time. Analysis of XRD results showed interaction between three parameters is the significant variable in determining the interlayer spacing of (002) crystalline planes. TEM images confirmed formation of ordered graphitic domains in the carbonized fibers mainly after 10 h of carbonization.

ACKNOWLEDGMENTS

The authors are thankful for the financial support from the Natural Sciences and Engineering Research Council (NSERC), Canada, for the Discovery grants individual Project #400320; NSERC NCE AUTO21 Project #460373; the Ontario Ministry of Economic Development and Innovation (MEDI) for the Ontario Research Fund (ORF) Research Excellence (RE) Round-4 Project #050289; and the Ontario Ministry of Agriculture, Food and Rural Affairs (OMAFRA)—University of Guelph Bioeconomy Industrial Uses Research Program Project #200371. The authors are also thankful to Lignol Innovations Ltd., Burnaby, British Columbia, Canada for providing the Organosolv Lignin samples for this research.

REFERENCES

1. Brosse, N.; Mohamad Ibrahim, M. N.; Abdul Rahim, A. *ISRN Mater. Sci.* **2011**, *2011*, 1.
2. Salehi Jouzani, G.; Taherzadeh, M. J. *Biofuel Res. J.* **2015**, *2*, 152.
3. Taherzadeh, M. J.; Karimi, K. *BioResources* **2007**, *2*, 707.
4. Zeng, Y.; Zhao, S.; Yang, S.; Ding, S. Y. *Curr. Opin. Biotechnol.* **2014**, *27*, 38.
5. Vishtal, A.; Kraslawski, A. *BioResources* **2011**, *6*, 3547.
6. Zhu, J. Y.; Pan, X. *J. Bioresource Technol.* **2010**, *101*, 4992.
7. Limayem, A.; Ricke, S. C. *Prog. Energy Combust. Sci.* **2012**, *38*, 449.
8. Silveira, M. H. L.; Morais, A. R. C.; da Costa Lopes, A. M.; Olekszyszen, D. N.; Bogel-Łukasik, R.; Andreaus, J.; Pereira Ramos, L. *ChemSusChem* **2015**, *8*, 3366.
9. Yang, B.; Wyman, C. E. *Biofuels Bioproducts Biorefining* **2008**, *2*, 26.
10. Thielemans, W.; Can, E.; Morye, S. S.; Wool, R. P. *J. Appl. Polym. Sci.* **2002**, *83*, 323.
11. Thielemans, W.; Wool, R. P. *Polym. Compos.* **2005**, *26*, 695.
12. Stanzione, J. F.; Giangiulio, P. A.; Sadler, J. M.; La Scala, J. J.; Wool, R. P. *ACS Sustainable Chem. Eng.* **2013**, *1*, 419.
13. Sannigrahi, P.; Pu, Y.; Ragauskas, A. *Curr. Opin. Environ. Sustainable* **2010**, *2*, 383.
14. Baker, D. A.; Rials, T. G. *J. Appl. Polym. Sci.* **2013**, *130*, 713.
15. Mainka, H.; Täger, O.; Körner, E.; Hilfert, L.; Busse, S.; Edelmann, F. T.; Herrmann, A. S. *J. Mater. Res. Technol.* **2015**, *4*, 283.
16. Chatterjee, S.; Jones, E. B.; Clingenpeel, A. C.; McKenna, A. M.; Rios, O.; McNutt, N. W.; Keffer, D. J.; Johs, A. *ACS Sustainable Chem. Eng.* **2014**, *2*, 2002.
17. Ramakrishna, S.; Fujihara, K.; Teo, W. E.; Lim, T. C.; Ma, Z. An Introduction to Electrospinning and Nanofibers; World Scientific Publishing Co. Pvt. Ltd.: Singapore, **2005**.
18. Ramakrishna, S.; Jose, R.; Archana, P.; Nair, A.; Balamurugan, R.; Venugopal, J.; Teo, W. *J. Mater. Sci.* **2010**, *45*, 6283.
19. Ma, X.; Elbohy, H.; Sigdel, S.; Lai, C.; Qiao, Q.; Fong, H. *RSC Adv.* **2016**, *6*, 11481.
20. Berenguer, R.; Garcia-Mateos, F. J.; Ruiz-Rosas, R.; Cazorla-Amoros, D.; Morallon, E.; Rodriguez-Mirasol, J.; Cordero, T. *Green Chem.* **2016**. *18*, 1506. DOI: 10.1039/C5GC02409A.
21. Lai, C.; Kolla, P.; Zhao, Y.; Fong, H.; Smirnova, A. L. *Electrochim. Acta* **2014**, *130*, 431.
22. Lai, C.; Zhou, Z.; Zhang, L.; Wang, X.; Zhou, Q.; Zhao, Y.; Wang, Y.; Wu, X. F.; Zhu, Z.; Fong, H. *J. Power Sources* **2014**, *247*, 134.
23. Hu, S.; Zhang, S.; Pan, N.; Hsieh, Y. L. *J. Power Sources* **2014**, *270*, 106.
24. Wang, S. X.; Yang, L.; Stubbs, L. P.; Li, X.; He, C. *ACS Appl. Mater. Interfaces* **2013**, *5*, 12275.
25. Choi, D.; Lee, J. N.; Song, J.; Kang, P. H.; Park, J. K.; Lee, Y. *J. Solid State Electrochem.* **2013**, *17*, 2471.
26. Dallmeyer, I.; Ko, F.; Kadla, J. F. *J. Wood Chem. Technol.* **2010**, *30*, 315.
27. Teng, N. Y.; Dallmeyer, I.; Kadla, J. F. *J. Wood Chem. Technol.* **2013**, *33*, 299.
28. Dallmeyer, I.; Chowdhury, S.; Kadla, J. F. *Biomacromolecules* **2013**, *14*, 2354.
29. Seo, D. K.; Jeun, J. P.; Kim, H. B.; Kang, P. H. *Rev. Adv. Mater. Sci.* **2011**, *28*, 31.
30. Xu, X.; Zhou, J.; Jiang, L.; Lubineau, G.; Chen, Y.; Wu, X. F.; Piere, R. *Mater. Lett.* **2013**, *109*, 175.
31. Ago, M.; Okajima, K.; Jakes, J. E.; Park, S.; Rojas, O. *J. Biomacromolecules* **2012**, *13*, 918.
32. Oroumei, A.; Fox, B.; Naebe, M. *ACS Sustainable Chem. Eng.* **2015**, *3*, 758.
33. Ding, R.; Wu, H.; Thunga, M.; Bowler, N.; Kessler, M. R. *Carbon* **2016**, *100*, 126.
34. Lallave, M.; Bedia, J.; Ruiz-Rosas, R.; Rodrí-Guez-Mirasol, J.; Cordero, T.; Otero, J. C.; Marquez, M.; Barrero, A.; Loscertales, I. G. *Adv. Mater.* **2007**, *19*, 4292.
35. Hu, S.; Hsieh, Y. L. *J. Mater. Chem. A* **2013**, *1*, 11279.
36. Poursorkhabi, V.; Mohanty, A. K.; Misra, M. *J. Appl. Polym. Sci.* **2015**, *132*, DOI: 10.1002/app.41260.
37. Salas, C.; Ago, M.; Lucia, L. A.; Rojas, O. *J. React. Funct. Polym.* **2014**, *85*, 221.
38. Foston, M.; Nunnery, G. A.; Meng, X.; Sun, Q.; Baker, F. S.; Ragauskas, A. *Carbon* **2013**, *52*, 65.
39. Frank, E.; Hermanutz, F.; Buchmeiser, M. R. *Macromol. Mater. Eng.* **2012**, *297*, 493.
40. Ruiz-Rosas, R.; Bedia, J.; Lallave, M.; Loscertales, I. G.; Barrero, A.; Rodríguez-Mirasol, J.; Cordero, T. *Carbon* **2010**, *48*, 696.
41. Schreiber, M.; Vivekanandhan, S.; Mohanty, A. K.; Misra, M. *ACS Sustainable Chem. Eng* **2015**, *3*, 33.
42. Dallmeyer, I.; Lin, L. T.; Li, Y.; Ko, F.; Kadla, J. F. *Macromol. Mater. Eng.* **2014**, *299*, 540.
43. Gao, G.; Ko, F.; Kadla, J. F. *Macromol. Mater. Eng.* **2015**, *300*, 836.
44. Youe, W. J.; Lee, S. M.; Lee, S. S.; Lee, S. H.; Kim, Y. S. *Int. J. Biol. Macromol.* **2016**, *82*, 497.

45. Liu, H. C.; Chien, A. T.; Newcomb, B. A.; Liu, Y.; Kumar, S. *ACS Sustainable Chem. Eng.* **2015**, *3*, 1943.

46. Braun, J. L.; Holtman, K. M.; Kadla, J. F. *Carbon* **2005**, *43*, 385.

47. Ma, Q.; Pyda, M.; Mao, B.; Cebe, P. *Polymer* **2013**, *54*, 2544.

48. Lee, S. C.; Han, J. I.; Jeong, Y. G.; Kwon, M. *Macromolecules* **2010**, *43*, 25.

49. Mainka, H.; Hilfert, L.; Busse, S.; Edelmann, F.; Haak, E.; Herrmann, A. S. *J. Mater. Res. Technol.* **2015**, *4*, 377.

50. Larouche, N.; Stansfield, B. L. *Carbon* **2010**, *48*, 620.

51. Tuinstra, F.; Koenig, J. L. *J. Compos. Mater.* **1970**, *4*, 492.

52. Jawhari, T.; Roid, A.; Casado, J. *Carbon* **1995**, *33*, 1561.

53. Paris, O.; Zollfrank, C.; Zickler, G. A. *Carbon* **2005**, *43*, 53.

54. Pimenta, M. A.; Dresselhaus, G.; Dresselhaus, M. S.; Cancado, L. G.; Jorio, A.; Saito, R. *Phys. Chem. Chem. Phys.* **2007**, *9*, 1276.

55. Cançado, L. G.; Takai, K.; Enoki, T.; Endo, M.; Kim, Y. A.; Mizusaki, H.; Jorio, A.; Coelho, L. N.; Magalhães-Paniago, R.; Pimenta, M. A. *Appl. Phys. Lett.* **2006**, *88*, 163106.

56. Keskar, G.; Rao, R.; Luo, J.; Hudson, J.; Chen, J.; Rao, A. M. *Chem. Phys. Lett.* **2005**, *412*, 269.

57. Deng, L.; Young, R. J.; Kinloch, I. A.; Zhu, Y.; Eichhorn, S. J. *Carbon* **2013**, *58*, 66.

58. Xu, X.; Zhou, J.; Jiang, L.; Lubineau, G.; Payne, S. A.; Gutschmidt, D. *Carbon* **2014**, *80*, 91.

59. Achyuthan, K. E.; Achyuthan, A. M.; Adams, P. D.; Dirk, S. M.; Harper, J. C.; Simmons, B. A.; Singh, A. K. *Molecules* **2010**, *15*, 8641.

60. Zussman, E.; Chen, X.; Ding, W.; Calabri, L.; Dikin, D. A.; Quintana, J. P.; Ruoff, R. S. *Carbon* **2005**, *43*, 2175.

61. Zhou, Z.; Liu, K.; Lai, C.; Zhang, L.; Li, J.; Hou, H.; Reneker, D. H.; Fong, H. *Polymer* **2010**, *51*, 2360.

62. Johnson, D. J.; Tomizuka, I.; Watanabe, O. *Carbon* **1975**, *13*, 321.